Microscopic Investigation of Shear in Multiwalled Nanotube Deformation

Ifat Kaplan-Ashiri,[†] Sidney R. Cohen,[‡] Nathan Apter,[‡] Yuekui Wang,[§] Gotthard Seifert,[§] H. Daniel Wagner,[†] and Reshef Tenne*[,†]

Department of Materials and Interfaces, Weizmann Institute of Science, Rehovot 76100, Israel, Department of Chemical Research Support, Weizmann Institute of Science, Rehovot 76100, Israel, and Institut für Physikalische Chemie, Technische Universität Dresden, D-01062, Germany

Received: January 31, 2007; In Final Form: April 17, 2007

The cylindrical geometry of nanotubes dictates a strong anisotropy of their physical properties. In practice, the difficulty in extracting individual components of the elastic tensor has limited the available information to only very partial and indirect experimental data. Here, the interlayer shear (sliding) modulus (C_{44}) of single multiwalled WS_2 nanotubes was studied by atomic force microscopy bending tests. The observed value of 2 GPa agrees well with the value of 4 GPa obtained for density functional tight binding calculations for 2H−MoS_2. This value of the shear modulus represents a much higher degree of anisotropy than that obtained for carbon nanotubes and enables assignment of the mode of shear deformation.

1. Introduction

The incorporation of nanotubes into various nanomechanical devices has highlighted the importance of understanding their behavior under stress. Several testing methods demonstrated in recent years have allowed direct investigation of the strength and elasticity of nanotubes and nanowires. These include pulling tests,[1−4] bending,[5−8] torsion,[9] and indirect methods.[10−13] The particular mechanical mode probed depends on the geometry of the fixed nanotube and extent of deformation. Thus, nanowires (tubes) have been modeled as elastic strings or as doubly clamped bending rods depending on the nanotube length/diameter ratio and ultimate bending configuration. In general, these high aspect ratio structures are highly anisotropic. Anisotropic materials exhibit directionally dependent properties, which can be attributed to the crystal structure (as in piezoelectric or layered materials). The anisotropy can also be the result of an induced structural effect (as in composite materials) or of the fabrication process (like cold working, spinning, etc.). Materials or structures with similar properties in one plane of symmetry are termed transversely isotropic.[14] They have five independent stiffness constants: C_{11}, C_{12}, C_{33}, C_{13}, and C_{44}. The elasticity matrix is[15,16]

$$C_{ij} = \begin{bmatrix} C_{11} & C_{12} & C_{13} & 0 & 0 & 0 \\ C_{12} & C_{11} & C_{13} & 0 & 0 & 0 \\ C_{13} & C_{13} & C_{33} & 0 & 0 & 0 \\ 0 & 0 & 0 & C_{44} & 0 & 0 \\ 0 & 0 & 0 & 0 & C_{44} & 0 \\ 0 & 0 & 0 & 0 & 0 & (C_{11} - C_{12})/2 \end{bmatrix} \quad (1)$$

The constants C_{11} and C_{12} characterize the Young's modulus and Poisson ratio in the symmetry plane (intralayer elastic moduli). The constants C_{33} and C_{13} characterize the Young's modulus and Poisson ratio perpendicular to this plane (interlayer elastic moduli). The constant C_{44} describes stresses caused by displacement of the layers with respect to each other.[15] Layered materials like graphite, WS_2, and MoS_2 are anisotropic with transversely isotropic symmetry.[15,17]

In contrast, the mechanical properties as well as the thermal and electrical properties of an isotropic material are similar in every direction. Isotropic materials can be mechanically characterized by three elastic constants: the modulus of elasticity, E; the shear modulus, G; and Poisson's ratio, ν. These constants are related by the isotropic relationship[18]

$$G = \frac{E}{2(1+\nu)} \quad (2)$$

Hence, there are only two independent elastic constants.

Individual single-wall and multiwalled carbon nanotubes as well as bundles have been treated as transversely isotropic materials.[19−21] Nevertheless, most of the studies on the mechanical properties of nanotubes were limited to the measurements and calculations of the Young's modulus (C_{11}) only.[20−22] Shen et al.[20,21] calculated five elastic moduli for both single-wall and multiwalled carbon nanotubes.

In the present study bending tests of individual multiwalled WS_2 nanotubes were performed in an atomic force microscope (AFM). The interlayer shear (sliding) modulus of the nanotubes was extracted from the bending equation and was found to be in good agreement with density functional tight binding (DFTB) calculation results of 2H-MoS_2.

2. Experimental Section

Multiwalled WS_2 nanotubes exhibiting high uniformity were synthesized in a fluidized bed reactor.[23,24] Their outer diameter varies from 10 to 30 nm, with the main size distribution centered around 15−20 nm. Furthermore, the inner radius is 6 nm and it varies very little from one nanotube to the other. These nanotubes have been shown to be quite perfectly crystalline and nearly defect free.[4]

* Corresponding author: tel, +972-8-9342394; fax, +972-8-9344138; e-mail, reshef.tenne@weizmann.ac.il.
[†] Department of Materials and Interfaces, Weizmann Institute of Science.
[‡] Department of Chemical Research Support, Weizmann Institute of Science.
[§] Institut für Physikalische Chemie, Technische Universität Dresden.

10.1021/jp070832k CCC: $37.00
Published on Web 05/27/2007

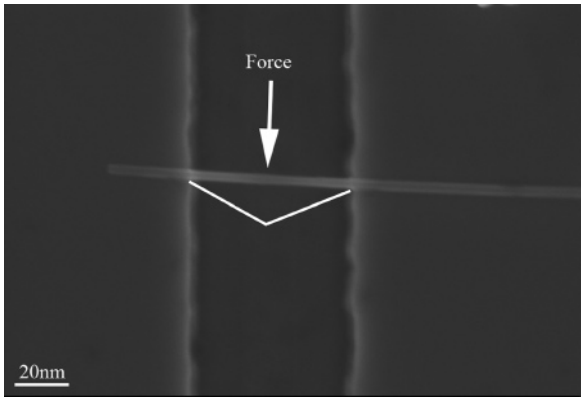

Figure 1. The experimental setup. A HRSEM micrograph of a WS_2 nanotube bridging a trench. The trenches were fabricated by e-beam lithography on GaAs substrate; they are 500 nm in width and 200−300 nm deep. The nanotube was bent by the AFM tip as described schematically by the white line.

The bending tests of individual WS_2 nanotubes were performed using the AFM according to a previously published procedure.[7,25] This method involves lateral manipulation of an individual nanotube which is mechanically fixed to and positioned over trenches on a GaAs substrate (Figure 1). Trenches were fabricated by electron-beam lithography and are 0.5−0.6 μm wide and 200−300 nm deep. The nanotubes were sonicated in ethanol for 5 min and then suspended over the GaAs substrate. Nanotubes that were found to span trenches in an orthogonal configuration by mapping with high-resolution scanning electron microscopy (HRSEM) were subsequently pinned down at the trench edges by exposing the contact point to the electron beam, producing amorphous carbon from hydrocarbons in the vacuum which forms a high strength glue.[26] The resulting structures were then subjected to lateral loading by an AFM cantilever under closed-loop control. With the tip cruising 70−100 nm above the plane of the substrate, the lateral deflection of the cantilever was monitored during the manipulation and the corresponding force-deflection ($F-d$) trace was recorded. The cantilever torsional force constant was calibrated according to the Sader torsional method.[27]

3. Calculations

Calculations of the sliding modulus were performed as follows:

The initial structure of a 6 × 6 supercell with 216 atoms was optimized using the experimental lattice parameters and the DFTB[28,29] plus dispersion[30] method. In this step the interlayer distance is reduced from 3.012 to 2.919 Å, which is mainly due to the DFTB approximation and not the van der Waals interactions.

To get the *minimum* energy structure for the van der Waals interactions, the interlayer distance L was reoptimized by a "rigid-shift" method, i.e., by calculating the DFTB and London dispersion energies as functions of L (or lattice parameter c) without structural relaxations. The optimized c value is 13.260 Å (see Figure 4), which is about 7.8% larger than the experimental value 12.295 Å. The corresponding interlayer distance is $L = 3.401$ Å.

To estimate the sliding modulus G for bulk 2H−MoS_2, the energy of the supercell obtained above was calculated by rigidly shifting the upper layer along the axis a step by step, while keeping c unchanged.

4. Results and Discussion

Clamped nanotubes were loaded laterally at the center of their suspended length by means of an AFM tip, and force vs lateral deflection ($F-d$) curves were recorded. The raw deflection data were separated into the cantilever torsional deflection and the sideways nanotube deflection. Notably, $F-d$ curves of the nanotubes exhibit a linear elastic behavior at small deflections (Figure 2a). The slope of the forward and backward-going curves is identical, notwithstanding a small offset due to piezo creep. $F-d$ curves with increasing bending deflections for a nanotube are presented in Figure 2b. Nonlinear deflection becomes evident when it exceeds 20 nm. These nonlinear curves at larger forces are elastic, as evidenced by congruency of successive curves. For the curves of highest deflection (63 and 97 nm), a discontinuity of the force appears but nonetheless the nanotube was not broken. This feature can be atrributed to a partial failure of the glue which holds the suspended nanotube to the underlying surface.

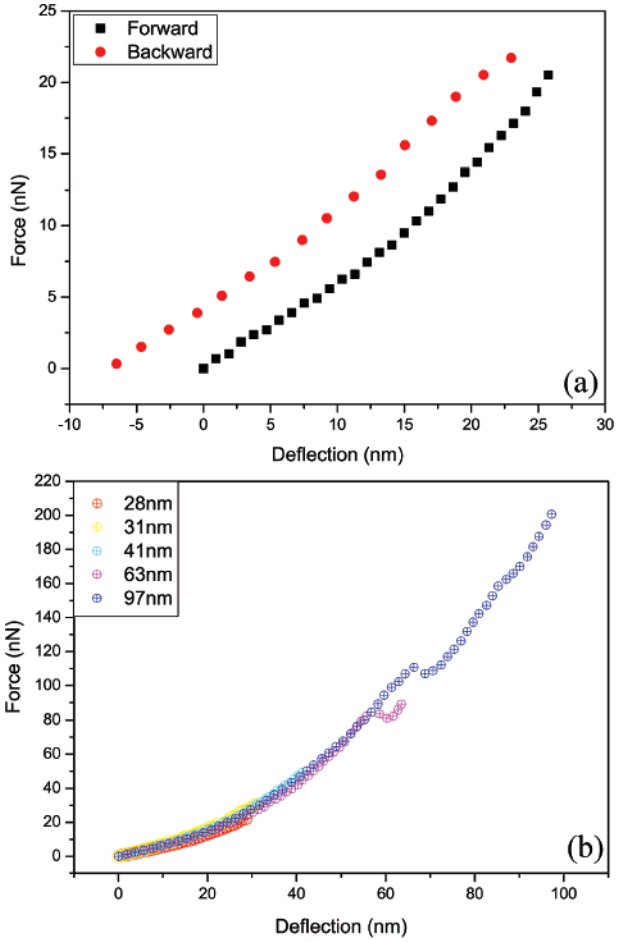

Figure 2. Force−deflection ($F-d$) curves: (a) $F-d$ curves of a nanotube in forward and backward directions. (b) $F-d$ curves of increasing deflection magnitude. One nanotube was bent several times, at successively larger deflections. The nanotube was not damaged during the experiment.

A clamped beam which is subjected to a point load can be described by Timoshenko's bending equation.[31] The total flexural deformation is composed of tension, compression, and shearing. Three-point bending configurations of thin stringlike specimens may be modeled with either pure bending[25] or pure stretching[7] analytical tools, depending on the mutual values of the anisotropy and span-to-depth ratio parameters. The regime of linear behavior under small loads, cited in the previous paragraph, indicates that limiting the deflections to 20 nm or less ensures that the behavior can be described as bending, and not stretching.[7] Hence, the total bending is composed of the bending deflection δ_b and the shear deflection δ_s, which are

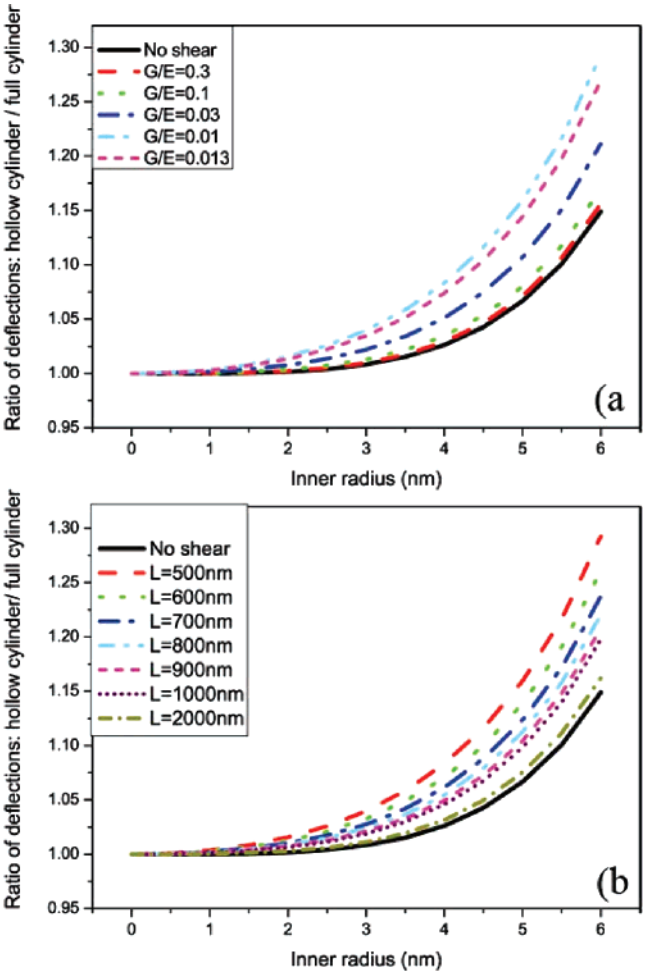

Figure 3. Calculated deflection ratio between a hollow cylinder and a full cylinder. (a) Deflection ratio for outer radius of 10 nm and length of 500 nm. The degree of anisotropy is represented by the ratio G/E—a value of 0.3 corresponds to the case of isotropic material, with the degree of anisotropy increasing for lower ratios. (b) Deflection ratio as calculated for $G/E = 0.01$, approximating the value determined here, for WS_2 at different suspended lengths. The outer radius was fixed at 10 nm.

linked to the bending stiffness (EI) and to the shear stiffness (GA), respectively. In order to calculate the Young's modulus from the $F-d$ curve, the shear modulus is required and vice versa.[32−34] The bending equation is[6,31]

$$\delta = \delta_b + \delta_s = \frac{FL^3}{192EI} + \frac{f_s FL}{4GA} \qquad (3)$$

Where δ is the nanotube's deflection, F is the applied lateral force, L is the suspended nanotube length, and E is the Young's modulus. I is the second moment of area (for a cylinder: $I = (\pi/4)(r_{out}^4 - r_{in}^4)$ where r_{out} and r_{in} are the outer and inner radii of the nanotube, respectively. f_s is the shape factor (10/9 for a cylinder), G is the shear modulus, and A the cross sectional area of the beam. The contribution of the shear stiffness to total deflection (second term in the right-hand side of eq 3) is a reflection, to a great extent, of the anisotropy of the material and of the geometrical characteristics of the specimen and is the focus of this study.[32−34] These effects are displayed by plotting the deflection ratio—the quotient of the deflection calculated from eq 3 for a hollow cylinder to that of a full cylinder—as a function of the inner radius (Figure 3a). This ratio grows both with the cylinder inner radius and, more significantly, with the degree of anisotropy (decreasing G/E), reaching 30% for $G/E = 0.01$. This contrasts with the case of isotropic materials ($G/E = 0.3$), where the shear contribution can be neglected.[18,31,35] The deflection ratio was further calculated for different cylinder lengths, for anisotropic material ($G/E = 0.01$). Figure 3b demonstrates that the shear action is responsible for approximately 25% of the deflection seen in these experiments.

TABLE 1: The Nanotubes' Radii and Their Corresponding Shear Moduli

nanotube's outer radius (nm)	nanotube's inner radius (nm)	the shear modulus (GPa)
15	6	2.24
12	6	1.08
10	6	2.22
14	6	2.17
13	6	1.47
10	6	0.88
10	6	4.32

The shear modulus G of the multiwalled WS_2 nanotubes was calculated for seven individual nanotubes according to eq 3. The $F-d$ data as obtained from the AFM, together with the nanotube dimensions measured by both HRSEM and AFM, were introduced into the bending equation. The previously determined Young's modulus value of 150 GPa[4,36] was used for the present analysis. The average shear modulus is 2.0 ± 1.1 GPa (the dimensions and the corresponding shear modulus for each nanotube are presented in Table 1). Therefore, $G/E = 0.013$ for WS_2 nanotubes, so that that the shear deformation must be taken into account when analyzing the results of the load point bending test.

As was mentioned above, transversely isotropic materials, like the nanotubes studied here can be described by five elastic moduli. The value of 2 GPa most probably corresponds to the interlayer shear (sliding) modulus (C_{44}).[15] From eq 2 and using values of 150 GPa (WS_2) and 230 GPa (MoS_2) for the Young's modulus,[36] one may conclude that the intralayer shear modulus (C_{12}) is 1 to 2 orders of magnitude higher. Indeed DFTB calculations showed that the intralayer shear moduli are 53 and 81.7 GPa for zigzag and armchair single wall MoS_2 nanotube, respectively.[37] This value is significantly different from C_{44} values previously determined from neutron data and X-ray measurements of the linear compressibilities for bulk 2H−MoS_2 (15 GPa)[17] and ropes of single wall MoS_2 nanotubes (0.16 GPa).[5] Those approximate values may differ from the more direct measurements presented here, although the low modulus of MoS_2 ropes[5] seems reasonable since interactions between different nanotubes in a rope would be smaller than the interlayer interactions between the walls within one nanotube where the conformity between sliding layers is dictated by the intertubular structure, rather than an interaction between different nanotubes.

Different models can be used to describe the shear process. The mechanism for shear deformation of a beam in a point load-bending test can be evaluated by considering thin cross-sectional elements which can slide relative to the adjacent ones.[31] This corresponds to "in-plane" (C_{12}) shear forces. Furthermore, in analogy to the case of the nanotubes, bending tests of sandwich materials made of alternating layers of hard and soft matter, result in a deformation which can be characterized by shearing of the soft layers.[16] In analogy to sandwich materials, the nanotubes can be regarded as being made of a superstructure of alternating hard (chemically bonded) WS_2 layers and soft interlayer spacing where weak van der Waals forces predominate. Hence, it is believed that the shear deformation of the nanotubes is obtained by slip between adjacent WS_2 layers. Layer slippage was studied for multiwalled carbon nanotubes

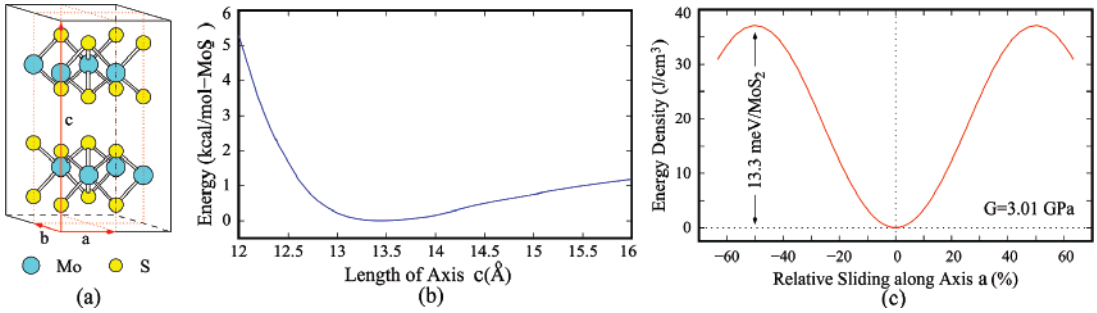

Figure 4. Crystal structure (a) and interlayer energies (b, c) of 2H−MoS_2: (a) 4 unit cells; (b) rigid shift of upper layer along *c*; (c) rigid shift of upper layer along *a*. (The energy at the minimum is set to zero.)

in pullout experiments,[3,38,39] and these forces were found to be very small. Sliding between individual nanotubes resulted in shear deformations for ropes of carbon[6] and MoS_2[5] single wall nanotubes.

To substantiate the assignment of measured shear to C_{44}, the sliding shear modulus of metal chalcogenide nanotubes (MoS_2, WS_2) was estimated by calculations of the sliding modulus of 2H−MoS_2, using the DFTB method.[28,29] Since the sliding occurred between the sulfur atoms of adjacent layers, and thus depends mostly on the interaction between neighboring S-layers, MoS_2 and WS_2 should have a similar sliding modulus (C_{44}). The results are plotted in Figure 4c. A plot of energy density versus the relative sliding parameter $\Delta a/a$ where a is the in-plane lattice parameter can be well approximated as

$$\frac{E}{V} = 35.13 \sin^2\left(\frac{\Delta a}{a}\pi\right)\left[1 + 0.06055 \sin^2\left(\frac{\Delta a}{a}\pi\right)\right] \approx 36.2 \sin^2\left(\frac{\Delta a}{a}\pi\right) \quad (4)$$

In units of J/cm^3. This relation is plotted in Figure 4c.

In accordance with this computational scheme, the sliding shear strain γ may be defined as

$$\gamma = \frac{\Delta a}{c/2} = 2\Delta a/c \quad (5)$$

where c is the length of the c axis and Δa is the sliding distance. On the basis of this definition, a polynomial fit of the energy densities to the sliding strain γ yields

$$G = \frac{1}{V}\frac{\partial^2 E}{\partial \gamma^2} = 4.09 \text{ GPa} \quad (6)$$

The total interlayer sliding modulus could be obtained by using the total energy (DFTB plus van der Waals energies). These first-principles values are in good agreement with the shear modulus measured here (2 GPa). The small difference can be attributed to structural differences between the calculated and measured systems: two layers of planar 2H−MoS_2 in the calculation vs the curved multiwalled nanotubes of WS_2 in the measurement.

5. Conclusions

In summary, the high degree of anisotropy for the multiwalled WS_2 nanotubes enabled direct measurement of the shear modulus under a three-point bending setup. Less anisotropic materials, such as single-walled carbon nanotubes, have no shear contribution under similar conditions. The shear component of the WS_2 nanotubes could be identified with slip motion between the different layers. This mode could be quite general for other types of multiwalled nanotubes. The experimental results can be compared favorably with first-principles calculations which indicate an easy shearing and sliding of the layers. The small interlayer shearing (sliding) modulus provides further evidence for the excellent tribological behavior of these materials, promoting numerous applications for these 1D nanomaterials.

Acknowledgment. We thank R. Rosentsveig for the synthesis of WS_2 nanotubes and M. Kokotov for the fabrication of trenches on the GaAs. This work was supported by the German−Israeli Foundation (GIF), the Minerva Foundation, and the G.M.J. Schmidt Minerva Center for Supramolecular Architectures. H. D. Wagner acknowledges the support of the NOESIS European project on "Aerospace Nanotube Hybrid Composite Structures with Sensing and Actuating Capabilities". H. D. Wagner is the recipient of the Livio Norzi Professorial Chair in Materials Science.

References and Notes

(1) Yu, M. F.; Lourie, O.; Dyer, M. J.; Moloni, K.; Kelly, T. F.; Ruoff, R. S. Strength and breaking mechanism of multiwalled carbon nanotubes under tensile load. *Science* **2000**, *287* (5453), 637−640.

(2) Yu, M. F.; Files, B. S.; Arepalli, S.; Ruoff, R. S. Tensile loading of ropes of single wall carbon nanotubes and their mechanical properties. *Phys. Rev. Lett.* **2000**, *84* (24), 5552−5555.

(3) Barber, A. H.; Cohen, S. R.; Wagner, H. D. Measurement of carbon nanotube-polymer interfacial strength. *Appl. Phys. Lett.* **2003**, *82* (23), 4140−4142.

(4) Kaplan-Ashiri, I.; Cohen, S. R.; Gartsman, K.; Ivanovskaya, V.; Heine, T.; Seifert, G.; Wiesel, I.; Wagner, H. D.; Tenne, R. On the mechanical behavior of WS_2 nanotubes under axial tension and compression. *Proc. Natl. Acad. Sci. U.S.A.* **2006**, *103* (3), 523−528.

(5) Kis, A.; Mihailovic, D.; Remskar, M.; Mrzel, A.; Jesih, A.; Piwonski, I.; Kulik, A. J.; Benoit, W.; Forro, L. Shear and Young's moduli of MoS_2 nanotube ropes. *Adv. Mater* **2003**, *15* (9), 733−736.

(6) Salvetat, J. P.; Briggs, G. A. D.; Bonard, J. M.; Bacsa, R. R.; Kulik, A. J.; Stockli, T.; Burnham, N. A.; Forro, L. Elastic and shear moduli of single-walled carbon nanotube ropes. *Phys. Rev. Lett.* **1999**, *82* (5), 944−947.

(7) Walters, D. A.; Ericson, L. M.; Casavant, M. J.; Liu, J.; Colbert, D. T.; Smith, K. A.; Smalley, R. E. Elastic strain of freely suspended single-wall carbon nanotube ropes. *Appl. Phys. Lett.* **1999**, *74* (25), 3803−3805.

(8) Duan, X. J.; Zhang, J.; Ling, X.; Liu, Z. F. Nano-welding by scanning probe microscope. *J. Am. Chem. Soc.* **2005**, *127* (23), 8268−8269.

(9) Williams, P. A.; Papadakis, S. J.; Patel, A. M.; Falvo, M. R.; Washburn, S.; Superfine, R. Torsional response and stiffening of individual multiwalled carbon nanotubes. *Phys. Rev. Lett.* **2002**, *89* (25), 255502.

(10) Treacy, M. M. J.; Ebbesen, T. W.; Gibson, J. M. Exceptionally high Young's modulus observed for individual carbon nanotubes. *Nature* **1996**, *381* (6584), 678−680.

(11) Chopra, N. G.; Zettl, A. Measurement of the elastic modulus of a multi-wall boron nitride nanotube. *Solid State Commun.* **1998**, *105* (5), 297−300.

(12) Wood, J. R.; Frogley, M. D.; Meurs, E. R.; Prins, A. D.; Peijs, T.; Dunstan, D. J.; Wagner, H. D. Mechanical response of carbon nanotubes under molecular and macroscopic pressures. *J. Phys. Chem. B* **1999**, *103* (47), 10388−10392.

(13) Frogley, M. D.; Zhao, Q.; Wagner, H. D. Polarized resonance Raman spectroscopy of single-wall carbon nanotubes within a polymer under strain. *Phys. Rev. B* **2002**, *65* (11), 113413.

(14) Kaw, A. K. *Mechanics of composite materials*; CRC Press: Boca Raton, FL, 1997; p 329.

(15) Abdullaev, N. A. Elastic properties of layered crystals. *Phys. Solid State* **2006**, *48* (4), 663−669.

(16) Vinson, J. R.; NetLibrary Inc., *The behavior of sandwich structures of isotropic and composite materials*; Technomic Publishing Co.: Lancaster, PA, 1999; pp xvi, 378.

(17) Feldman, J. L. Elastic-Constants of 2H-MoS_2 and 2H-$NbSe_2$ Extracted from Measured Dispersion Curves and Linear Compressibilities. *J. Phys. Chem. Solids* **1976**, *37* (12), 1141−1144.

(18) Gere, J. M. *Mechanics of materials*, 6th ed.; Brooks/Cole: Pacific Grove, CA, and London, 2004; pp xx, 940.

(19) Saether, E.; Frankland, S. J. V.; Pipes, R. B. Transverse mechanical properties of single-walled carbon nanotube crystals. Part I: determination of elastic moduli. *Compos. Sci. Technol.* **2003**, *63* (11), 1543−1550.

(20) Shen, L. X.; Li, J. Transversely isotropic elastic properties of single-walled carbon nanotubes. *Phys. Rev. B* **2004**, *69* (4), 045414.

(21) Shen, L. X.; Li, J. Transversely isotropic elastic properties of multiwalled carbon nanotubes. *Phys. Rev. B* **2005**, *71* (3), 035412.

(22) Yakobson, B. I.; Avouris, P. Mechanical properties of carbon nanotubes. *Carbon Nanotubes* **2001**, *80*, 287−327.

(23) Rosentsveig, R.; Margolin, A.; Feldman, Y.; Popovitz-Biro, R.; Tenne, R. Bundles and foils of WS_2 nanotubes. *Appl. Phys. A: Mater. Sci. Process.* **2002**, *74* (3), 367−369.

(24) Rosentsveig, R.; Margolin, A.; Feldman, Y.; Popovitz-Biro, R.; Tenne, R. WS_2 nanotube bundles and foils. *Chem. Mater* **2002**, *14* (2), 471−473.

(25) Wu, B.; Heidelberg, A.; Boland, J. J. Mechanical properties of ultrahigh-strength gold nanowires. *Nat. Mater* **2005**, *4* (7), 525−529.

(26) Ding, W.; Dikin, D. A.; Chen, X.; Piner, R. D.; Ruoff, R. S.; Zussman, E.; Wang, X.; Li, X. Mechanics of hydrogenated amorphous carbon deposits from electron-beam-induced deposition of a paraffin precursor. *J. Appl. Phys.* **2005**, *98* (1), 014905.

(27) Green, C. P.; Lioe, H.; Cleveland, J. P.; Proksch, R.; Mulvaney, P.; Sader, J. E. Normal and torsional spring constants of atomic force microscope cantilevers. *Rev. Sci. Instrum.* **2004**, *75* (6), 1988−1996.

(28) Porezag, D.; Frauenheim, T.; Kohler, T.; Seifert, G.; Kaschner, R. Construction of Tight-Binding-Like Potentials on the Basis of Density-Functional Theory-Application to Carbon. *Phys. Rev. B* **1995**, *51* (19), 12947−12957.

(29) Seifert, G.; Porezag, D.; Frauenheim, T. Calculations of molecules, clusters, and solids with a simplified LCAO-DFT-LDA scheme. *Int. J. Quantum Chem.* **1996**, *58* (2), 185−192.

(30) Zhechkov, L.; Heine, T.; Patchkovskii, S.; Seifert, G.; Duarte, H. A. An efficient a Posteriori treatment for dispersion interaction in density-functional-based tight binding. *J. Chem. Theory Comput.* **2005**, *1* (5), 841−847.

(31) Timoshenko, S. *Strength of materials*, 3d ed.; Van Nostrand: New York, 1955; p 2v.

(32) Fischer, S.; Roman, I.; Harel, H.; Marom, G.; Wagner, H. D. Simultaneous Determination of Shear and Youngs Moduli in Composites. *J. Test. Eval.* **1981**, *9* (5), 303−307.

(33) Wagner, H. D.; Fischer, S.; Roman, I.; Marom, G. The Effect of Fiber Content on the Simultaneous Determination of Young and Shear Moduli of Unidirectional Composites. *Composites* **1981**, *12* (4), 257−259.

(34) Wagner, H. D.; Marom, G.; Roman, I. Analysis of Several Loading Methods for Simultaneous Determination of Young and Shear Moduli in Composites. *Fibre Sci. Technol.* **1982**, *16* (1), 61−65.

(35) Barbero, E. J. *Introduction to composite materials design*; Taylor and Francis: Philadelphia, PA, 1999; pp xvii, 336.

(36) Kaplan-Ashiri, I.; Cohen, S. R.; Gartsman, K.; Rosentsveig, R.; Seifert, G.; Tenne, R. Mechanical behavior of individual WS_2 nanotubes. *J. Mater. Res.* **2004**, *19* (2), 454−459.

(37) Seifert, G. Unpublished results.

(38) Cumings, J.; Zettl, A. Low-friction nanoscale linear bearing realized from multiwall carbon nanotubes. *Science* **2000**, *289* (5479), 602−604.

(39) Yu, M. F.; Yakobson, B. I.; Ruoff, R. S. Controlled sliding and pullout of nested shells in individual multiwalled carbon nanotubes. *J. Phys. Chem. B* **2000**, *104* (37), 8764−8767.